

Induced Gravitational Waves probing Primordial Black Hole Dark Matter with Memory Burden

Kazunori Kohri^{a,b,c,d}, Takahiro Terada^{e,f}, and Tsutomu T. Yanagida^{d,g}

^a *Division of Science, National Astronomical Observatory of Japan, Mitaka, Tokyo 181-8588, Japan*

^b *The Graduate University for Advanced Studies (SOKENDAI), Mitaka, Tokyo 181-8588, Japan*

^c *Theory Center, IPNS, and QUP (WPI), KEK, 1-1 Oho, Tsukuba, Ibaraki 305-0801, Japan*

^d *Kavli IPMU (WPI), UTIAS, The University of Tokyo, Kashiwa, Chiba 277-8583, Japan*

^e *Kobayashi-Maskawa Institute for the Origin of Particles and the Universe, Nagoya University, Tokai National Higher Education and Research System, Furo-cho Chikusa-ku, Nagoya 464-8602, Japan*

^f *TRIP Headquarters, RIKEN, Wako 351-0198, Japan*

^g *Tsung-Dao Lee Institute & School of Physics and Astronomy, Shanghai Jiao Tong University, Pudong New Area, Shanghai 201210, China*

Abstract

Quantum evaporation of a black hole is conventionally studied semiclassically by assuming self-similarity of the black hole throughout the evaporation process. However, its validity was recently questioned, and the lifetime of a black hole is conjectured to be much extended by the memory burden effect. It gives rise to the possibility that the primordial black holes (PBHs) *lighter* than 10^{10} grams are the dark matter in the Universe. To probe such PBH dark matter, we study gravitational waves (GWs) induced by primordial curvature perturbations that produced the PBHs. We find $\Omega_{\text{GW}}(f_{\text{peak}})h^2 = 7 \times 10^{-9}$ with the peak frequency $f_{\text{peak}} = 1 \times 10^3 (M_{\text{PBH}}/(10^{10} \text{ g}))^{-1/2}$ Hz, and the induced GWs associated with the PBH dark matter whose initial mass is greater than about 10^7 grams can be tested by future observations such as Cosmic Explorer. Furthermore, the scenario can be in principle confirmed by detecting another GW signal from the mergers of PBHs, which leads to high-frequency GWs with $f_{\text{peak}} = 2 \times 10^{27} (M_{\text{PBH, ini}}/(10^{10} \text{ g}))^{-1}$ Hz. On the other hand, the induced GW signals stronger than expected would contradict the dark matter abundance and exclude the memory burden effect.

1 Introduction

Primordial black holes (PBHs) are one of the leading candidates of cold dark matter other than elementary particles. They are classically stable, but they evaporate by the quantum effect emitting Hawking radiation [1, 2]. The lifetime scales as $M_{\text{PBH,ini}}^3/M_{\text{P}}^4$ where $M_{\text{PBH,ini}}$ is the initial mass of the PBH and M_{P} is the reduced Planck mass, so the PBHs heavier than about 10^{15} gram can survive until today to be the dark matter in the Universe [3]. We refer the readers to reviews [4–7] for the status of PBHs as a dark matter candidate.

The above conventional picture is based on the semiclassical calculation [2], in which quantum fields for radiation degrees of freedom are treated on the fixed classical black-hole geometry. Apparently, this makes sense for a sufficiently heavy black hole since the backreaction should be small at each moment. Though it is a small effect, the black hole gradually loses its mass. Then, one can study the Hawking emission process with a black-hole mass a bit smaller than the initial value. Supported by the no-hair theorem [8, 9], one usually assumes the self-similarity of the problem. Namely, one repeats the same argument even when the mass of the black hole significantly changes. It is usually assumed that the evaporation continues at least until the black hole becomes as light as the Planck mass, so knowledge about quantum gravity is necessary. This leads to the information loss paradox [10], which itself is not our main interest in this paper. Rather, we discuss the cosmological consequences of the potential breakdown of self-similarity and the semiclassical calculation well before reaching the Planck scale.

In series of papers [11–21], Dvali and his collaborators developed the following picture, in which PBHs are effectively stabilized against Hawking evaporation. First, a black hole can be understood as a condensate of a large number of soft gravitons [11–13]. A crucial assumption is that these soft modes interact with hard modes in such a way that once a critical number of the soft modes is populated, a large number of hard modes gets gapless. This phenomenon is called assisted gaplessness [15–18]. The soft mode controls the energy level of the hard modes, so the former is also called the master mode. The hard modes can encode an exponential amount of information and are also called memory modes, which are mostly responsible for the entropy of the black hole. A typical microstate of the memory modes contains a large excitation number of gapless modes, whose energy level depends on the excitation number of the master mode. This means that the memory modes backreact on the master mode dynamics since the change of the master mode population would cost huge energy [19, 20]. The slogan is then a black hole, or more generally, any system with large memory modes is effectively stabilized by the burden of its memory. The effect gets important when the black hole loses an $\mathcal{O}(1)$ fraction of its initial mass. Quantitatively, they claimed that this occurs at the latest when the black hole loses half of its initial mass [20]. That is, an older black hole that emitted more than half of its initial mass is not equivalent to a young black hole with the same mass, violating the self-similarity.

After the memory burden effect becomes important, the precise behavior of the black hole is not clear. Dvali et al. proposed either of the following possibilities occur [19, 20]: (i) the Hawking emission rate is significantly suppressed, or (ii) a new classical instability comes in so that the black hole decays into some lumps and gravitational waves. The first possibility opens up a new allowed window for the PBH dark matter mass [19, 20, 22, 23], so we focus on this possibility.¹ Quantitatively, Dvali et al. argued that the Hawking emission rate is suppressed by some integer power n_{MB} [defined in Eq. (5) below] of its entropy S_{BH} [19, 20, 22]. As the black hole entropy is huge, $S_{\text{BH}} \gg 1$, the lifetime of a black hole is significantly extended. However, black holes do evaporate with a suppressed Hawking-emission rate, so we are not considering the absolutely stable remnants of black hole evaporation.²

Cosmological constraints on PBHs beyond the semiclassical regime, i.e., with the memory burden effect were studied in Refs. [22, 23]. In particular, Ref. [23] showed the upper bound on the initial PBH mass of $M_{\text{PBH,ini}} \lesssim 10^{10}$ g from big bang nucleosynthesis (BBN) while the

¹Dark matter can be PBHs in this case but does not have to be so. Dark matter parameter space in the presence of memory-burden PBHs was studied in Refs. [24, 25].

²They are in tension with the covariant entropy bound [26]. For an extended discussion on remnants, see Ref. [27]. Induced GWs to probe black hole remnants were studied in Ref. [28].

lower bound from galactic and extragalactic gamma rays [4, 29] depends on the suppression power n_{MB} of the memory burden effect. For $n_{\text{MB}} = 1$, the allowed region is almost closed. For $n_{\text{MB}} = 2$, the allowed mass is $10^5 \text{ g} \lesssim M_{\text{PBH,ini}} \lesssim 10^{10} \text{ g}$. While $n_{\text{MB}} > 2$ allows lighter PBHs and this extension is straightforward, the associated induced GWs have too high frequencies to be detected in the near future. Assuming the post-inflationary PBH formation mechanism in the radiation-dominated era [30, 31], the lower bound on the PBH mass is $M_{\text{PBH,ini}} \gtrsim 0.5 \text{ g}$, which comes from the upper bound on the tensor-to-scalar ratio $r \lesssim 0.04$ [32–34] with the measured amplitude of the primordial curvature perturbations $A_s = 2.1 \times 10^{-9}$ [35, 36]. Therefore, we consider the mass range $0.5 \text{ g} \lesssim M_{\text{PBH,ini}} \lesssim 10^{10} \text{ g}$ but focus on $10^5 \text{ g} \lesssim M_{\text{PBH,ini}} \lesssim 10^{10} \text{ g}$.

As pointed out in Refs. [37, 38], the PBH scenario may well be associated with GWs induced by the primordial curvature perturbations. This is because, in a popular PBH production mechanism, it is produced by the gravitational collapse of a cosmological patch with extremely enhanced curvature perturbations [30, 31]. The latter necessarily induces a significant intensity of gravitational waves beyond the linear order of the cosmological perturbation theory [39–44]. It is useful to note that the initial PBH mass and the typical frequency of the induced GWs are in one-to-one correspondence. In the conventional scenario without the memory burden effect, the asteroid-mass PBHs can constitute 100% abundance of the dark matter, whose corresponding induced GWs can be probed by a space-based GW interferometer [37, 38] such as Laser Interferometer Space Antenna (LISA) [45, 46].

In this paper, we study the induced GWs associated with the PBH dark matter in the presence of the memory burden effect. Our focus is the simple scenario in which the induced GWs are produced around the time of PBH formation in the radiation-dominated era.³ In section 2, we review PBHs discussing their formation, evaporation, and abundance in the presence of the memory burden effect. We introduce example power spectra of the primordial curvature perturbations. Section 3 is the main section of this paper, where we discuss the induced-GW signals of the memory-burdened PBH dark matter scenario. We discuss the observational prospects of the induced GWs. In Section 4, we discuss some possibilities to cross-check or exclude the memory-burdened PBH dark matter scenario. For example, we argue that the memory burden effect can be excluded if the induced GWs associated with the light PBHs are too strong. We also discuss another GW signal, which is from mergers of PBHs, to confirm the memory burden effect although the frequency of the GWs is extremely high. We summarize the paper and conclude in section 5. We use the natural unit $c = \hbar = k_{\text{B}} = 8\pi G = 1$ unless explicitly denoted.

2 Primordial black hole abundance with memory burden

In this section, we summarize our method of calculation of the PBH abundance and mention some differences from the conventional case without the memory burden effect.

Although the PBH abundance is sensitive to the details of the calculation method,⁴ the difference can be absorbed by the amplitude of the curvature perturbations. Since the PBH abundance is extremely sensitive to it while the intensity of the induced GWs, which is the main topic of this paper, is only quadratically sensitive, our results do not depend on the details of the

³Recently, another induced-GW signal related to the *non*-dark-matter PBHs was studied in Ref. [25, 47, 48]. In their scenario, PBHs dominate the Universe and then evaporate to reheat the Universe. If the distributions of the mass and spin of PBHs are negligible, the PBHs evaporate almost simultaneously leading to a rapid change of the equation of state of the Universe. In such an occasion, the induced GWs are significantly enhanced by the poltergeist mechanism [49] (named in Ref. [50]), where the perturbations (of the PBH number density [50]) were assumed to be adiabatic. It was generalized to the Poissonian case [51] in Ref. [52]. The Poissonian contribution was considered in Refs. [25, 47], while both contributions were considered in Ref. [48]. See also Refs. [50, 53–56] for the importance of the finite transition time scale, which makes the enhancement of the induced GWs milder. Note also that the mass distribution of the memory-burden PBHs was discussed in Ref. [21], which suppresses the induced GWs from the poltergeist mechanism [50, 54].

⁴See Refs. [57–62] for recent discussions on (uncertainties of) the PBH abundance. For more general reviews of PBHs, see Refs. [4, 5, 7, 63].

calculation formalism of the PBH abundance. Therefore, we take a simple method; we basically follow the method in Refs. [57, 64–66].⁵

We consider PBH formation in a radiation-dominated epoch. The (initial) mass of a PBH created in a Hubble patch with enhanced curvature perturbations is given by a fraction γ of the Hubble horizon mass

$$M_{\text{PBH,ini}} = \frac{4\pi\gamma}{3} H^{-3}, \quad (1)$$

where H is the Hubble parameter, which is related via $H = k/a$ to the wavenumber k of the fluctuation with a being the scale factor of the Friedmann–Lemaître–Robertson–Walker metric. We take $\gamma = (1/\sqrt{3})^3$ [67].

Carr’s formula [67] (cf. the Press-Schechter formalism [68]) for the PBH formation probability β is

$$\beta(M) = \frac{1}{2} \text{Erfc} \left(\frac{\delta_c}{\sqrt{2\sigma^2(k)}} \right), \quad (2)$$

where Erfc denotes the complementary error function, δ_c is the critical overdensity to form a PBH, and $\sigma^2(k)$ is the variance of the coarse-grained overdensity:

$$\sigma^2(k) = \frac{16}{81} \int_{-\infty}^{\infty} d \ln q \left(\frac{q}{k} \right)^4 W \left(\frac{q}{k} \right)^2 T \left(\frac{q}{k} \right)^2 \mathcal{P}_\zeta(q), \quad (3)$$

where $W(z)$ is the window function, for which we take $W(z) = \exp(-z^2/2)$, $T(z) = 9\sqrt{3}(\sin(z/\sqrt{3}) - z/\sqrt{3} \cos(z/\sqrt{3}))/z^3$ is the transfer function, and $\mathcal{P}_\zeta(k)$ is the dimensionless power spectrum of the primordial curvature perturbations.

In this paper, we consider two types of $\mathcal{P}_\zeta(k)$ for illustrative purposes. One is the delta function and the other is Gaussian in terms of $\ln k$.

$$\mathcal{P}_\zeta(k) = \begin{cases} A_\zeta \delta \left(\ln \frac{k}{k_0} \right) \\ \frac{A_\zeta}{\sqrt{2\pi\Delta^2}} \exp \left(-\frac{\left(\ln \frac{k}{k_0} \right)^2}{2\Delta^2} \right) \end{cases} \quad (4)$$

where k_0 is a reference scale, A_ζ is the amplitude of the curvature perturbations, and Δ is the width of the Gaussian. Note that the delta-function case is the $\Delta \rightarrow 0$ limit of the lognormal case. An advantage of the delta function $\mathcal{P}_\zeta(k)$ is that the resulting PBH mass function is as narrow as possible so that the comparison to observational constraints (usually derived by assuming the monochromatic PBH mass function) is relatively straightforward. A disadvantage of the delta-function case is that model building to realize such a narrow limit of \mathcal{P}_ζ is nontrivial. On the other hand, an advantage of the lognormal $\mathcal{P}_\zeta(k)$ is that it can approximate realistic smooth spectra. A disadvantage, however, is that the resulting PBH mass function is broader, so the comparison to PBH constraints becomes nontrivial. Thus, the two options of $\mathcal{P}_\zeta(k)$ are complementary.

To discuss the PBH abundance at present, we need to discuss Hawking radiation and the memory burden effect. The mass loss rate by the Hawking radiation is given by (see Refs. [69–71] for the case without the memory burden effect)

$$\dot{M}_{\text{PBH}} = \begin{cases} -\frac{\pi\mathcal{G}g_{*H}}{480M_{\text{PBH}}^2} & (M_{\text{PBH}} \geq qM_{\text{PBH,ini}}) \\ -\frac{\pi\mathcal{G}g_{*H}}{480S_{\text{BH}}^{n_{\text{MB}}} M_{\text{PBH}}^2} & (M_{\text{PBH}} < qM_{\text{PBH,ini}}) \end{cases} \quad (5)$$

where $\mathcal{G} \simeq 3.8$ is the gray-body factor, $g_{*H} (\simeq 108$ for $M_{\text{PBH}} \ll 10^{11}$ g in the Standard Model [69] at least in the conventional case without memory burden) is the effective number of degrees of

⁵The differences are as follows. We use $\delta_c = 0.42$ rather than 0.45. This means that PBHs are more easily produced. To adjust the PBH abundance, a smaller amplitude of the curvature perturbations is required. This leads to a conservative estimate for the induced GWs. We also use $\gamma = (1/\sqrt{3})^3$ rather than 0.2 following Ref. [67].

freedom emitted by Hawking radiation, and $1/2 \leq q \leq 1$ parameterizes the critical mass at which the memory burden effect becomes relevant. The Bekenstein-Hawking entropy of the black hole is given by $S_{\text{BH}}(M_{\text{PBH}}) = 2\pi A = M_{\text{PBH}}^2/2$ [2, 72] in the reduced Planck unit with $A = M_{\text{PBH}}^2/(4\pi)$ being the surface area. There are some caveats in the above expression. First, the detailed form of the emission rate in the memory-burden regime is unknown. Beyond the semiclassical regime, it is not clear if we can rely on notions of the black-hole thermodynamics [73] such as Hawking temperature and entropy. Second, the above evaporation rate is discontinuous at $M_{\text{PBH}} = qM_{\text{PBH,ini}}$. Realistically, the evaporation rate will smoothly transform from the semiclassical regime to the memory burden regime because the magnitude of the backreaction from the memory modes to the master mode is continuous. Third, there are several proposals [22, 23, 47] for the detailed form of the evaporation rate in the memory burden regime. For example, some authors replace M_{PBH} and/or $S_{\text{BH}}(M_{\text{PBH}})$ with $qM_{\text{PBH,ini}}$ and/or $S_{\text{BH}}(qM_{\text{PBH,ini}})$. These differences lead to only negligible effects on observables at present at least in the parameter range of our main interest $10^5 \leq M_{\text{PBH,ini}}/g \leq 10^{10}$. For $n_{\text{MB}} \geq 2$, it is a good approximation to set $M_{\text{PBH}}|_{\text{present}} = qM_{\text{PBH,ini}}$ since the Hawking emission rate in the semiclassical regime for these masses is so effective while the evaporation rate is significantly suppressed in the memory burden regime.

The present abundance of PBHs is that in the conventional case times the fraction q for the parameter range of our main interest

$$f_{\text{PBH}} \equiv \frac{\rho_{\text{PBH}}}{\rho_{\text{CDM}}} = q \int_{-\infty}^{\infty} d \ln M \frac{g_*(T(M))}{g_{*,0}} \frac{g_{*s,0}}{g_{*s}(T(M))} \frac{T(M)}{T_{\text{eq}}} \gamma\beta(M) \frac{\Omega_{\text{m}}}{\Omega_{\text{CDM}}}, \quad (6)$$

where $g_*(T)$ and $g_{*s}(T)$ are the effective number of relativistic degrees of freedom for energy density and entropy density, respectively, $T(M)$ is the temperature at the formation of PBH with its (initial) mass M , T_{eq} is the temperature at the matter-radiation equality, and $\Omega_X = \rho_X/\rho_{\text{total}}$ is the energy-density fraction of component X (m: matter, CDM: cold dark matter, r: radiation, etc.). In the following, we fix $q = 1/2$ for definiteness. We use the numerical fitting functions in Ref. [74] for $g_*(T)$ and $g_{*s}(T)$.

3 Induced gravitational waves

The memory burden effect changes the relation between the initial PBH mass $M_{\text{PBH,ini}}$ and its present value M_{PBH} , but the relation between the PBH formation and the induced GWs is unaffected. The enhanced primordial curvature perturbations responsible for the PBH formation also produce GWs secondarily via interactions in General Relativity. Although the leading-order contribution to the induced GWs is the second order, it can dominate over the first-order GWs produced during inflation directly from tensor-field vacuum fluctuation without violating perturbativity. This is because the source of the first-order (primordial) GWs and the second-order (induced) GWs are different.

The spectrum of the scalar-induced GWs is obtained as [43, 44, 75, 76]

$$\Omega_{\text{GW}}(\eta_0, f)h^2 = \frac{g_*(T(f))}{g_{*,0}} \left(\frac{g_{*s,0}}{g_{*s}(T(f))} \right)^{4/3} \Omega_{\text{r}} h^2 \Omega_{\text{GW}}(\eta_c, f), \quad (7)$$

$$\Omega_{\text{GW}}(\eta_c, f) = \frac{1}{6} \int_0^\infty dt \int_0^1 ds \left(\frac{t(2+t)(s^2-1)}{(1-s+t)(1+s+t)} \right)^2 \lim_{\eta \rightarrow \infty} \overline{(k\eta)^2 I(t, s, k\eta)^2} \mathcal{P}_\zeta(uk) \mathcal{P}_\zeta(vk), \quad (8)$$

where η is the conformal time, $h = H_0/(100 \text{ km/s/Mpc})$ is the reduced Hubble parameter, $k = 2\pi f$ is the wavenumber of the GWs, $\Omega_{\text{GW}}(\eta_c)$ is the value of $\Omega_{\text{GW}}(\eta)$ that reached a constant value during the radiation-dominated epoch, $u = (t+s+1)/2$, $v = (t-s+1)/2$, and the oscillation average (denoted by the overline) of the kernel function $\lim_{\eta \rightarrow \infty} \overline{(k\eta)^2 I(t, s, k\eta)^2}$ is [75, 76]

$$\lim_{\eta \rightarrow \infty} \overline{(k\eta)^2 I(t, s, k\eta)^2} = \frac{288(-5+s^2+t(2+t))^2}{(1-s+t)^6(1+s+t)^6} \left(\frac{\pi^2}{4} (-5+s^2+t(2+t))^2 \Theta(t - (\sqrt{3}-1)) \right)$$

$$+ \left(-(t-s+1)(t+s+1) + \frac{1}{2} (-5 + s^2 + t(2+t)) \ln \left| \frac{t(2+t)-2}{3-s^2} \right| \right)^2, \quad (9)$$

where Θ is the Heaviside step function.

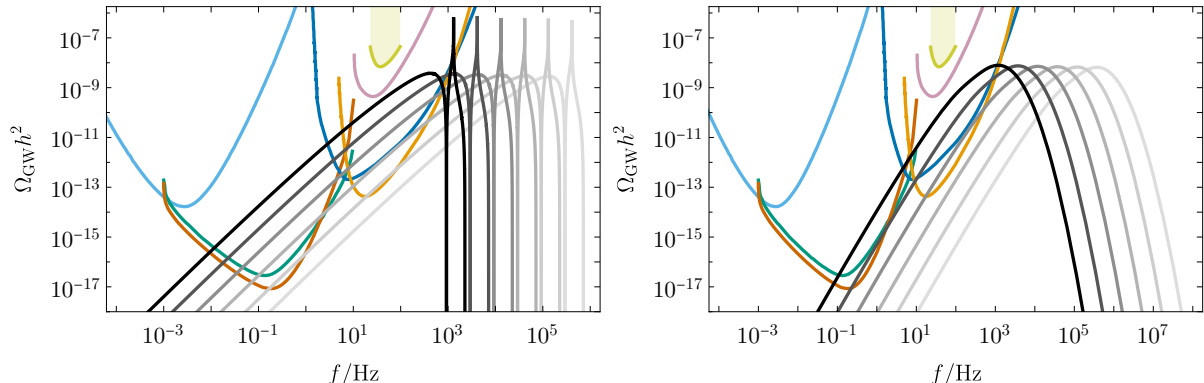


Figure 1: The spectra of the induced GWs are shown in monochrome colors. From left (black) to right (light gray), $M_{\text{PBH,ini}}/g = 10^{10}, 10^9, 10^8, 10^7, 10^6$, and 10^5 . The left and right panels show the cases with \mathcal{P}_ζ being the delta function and the lognormal function with $\Delta = 1$, respectively. The colored lines denote the power-law integrated sensitivity curves for 1-year observations adopted from Ref. [77]. The observations include LISA (sky blue), DECIGO (bluish green), BBO (vermilion), ET (blue), CE (orange), HLVK (design sensitivity) (reddish purple), and HLV O3 (yellow shaded).

The spectra of the induced GWs are plotted in Fig. 1 with the power-law integrated sensitivity curves of various GW observations assuming 1 year observations. The left panel shows the case of the delta-function $\mathcal{P}_\zeta(k)$, and the right panel shows the case of the lognormal $\mathcal{P}_\zeta(k)$. Since a small-scale mode re-enters the Hubble horizon earlier, the induced GWs associated with a smaller PBH have higher frequencies.

The largest difference between the delta-function case and the lognormal case is the power-law index of $\Omega_{\text{GW}}(f)$ on the infrared (IR) tail. The power-law index is 2 and 3 for the delta-function case and the lognormal case, respectively, up to a logarithmic correction [78]. The latter value 3 is the universal result based on causality and statistics with the assumption that the GWs are emitted in a finite duration in the radiation-dominated epoch [79]. For details, see also Ref. [80]. Because of the lightness of the memory-burdened PBH dark matter, the mainly observable part of the GW spectrum is the IR tail, whereas the peak height of the GW spectrum is approximately the same for both cases once we fit the PBH dark matter abundance ($f_{\text{PBH}} = 1$). Therefore, the induced GWs from the delta-function $\mathcal{P}_\zeta(k)$ can be more easily tested.

The power-law integrated sensitivity curves in Fig. 1 are those of the following GW observations. The sky blue, bluish green, and vermilion lines correspond to LISA [45, 46], DECihertz Interferometer Gravitational wave Observatory (DECIGO) [81–84], and Big Bang Observer (BBO) [85–87]. These are space-based interferometers. The shaded yellow region is the Laser Interferometer Gravitational-Wave Observatory (LIGO)/Virgo (HLV) O3 constraint on SGWB [88]. This is an existing constraint whereas the other lines are sensitivity curves for future observations taken from Ref. [77]. The pink line corresponds to a combination of advanced LIGO [89, 90], advanced Virgo [91], and Kamioka Gravitational wave detector (KAGRA) [92–96] (HLVK). These are ground-based interferometers. The next generation ground-based interferometers include Einstein Telescope (ET) [97–100] (the blue line) and Cosmic Explorer (CE) [101, 102] (the orange line).

Let us more quantitatively discuss the observational prospect. The IR tail of the GW spectrum approximately follows the power law, so the power-law integrated sensitivity curves are useful guides. However, the signals do not completely follow the power law. To be more precise, it is better to compute the signal-to-noise ratio (SNR) without assuming the power law.

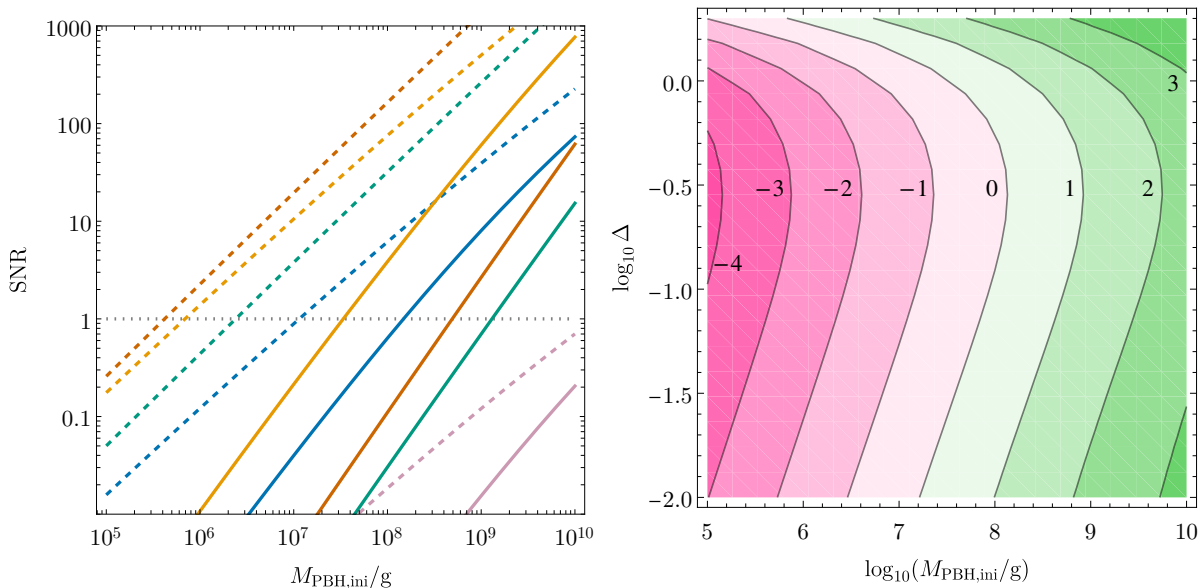


Figure 2: The signal-to-noise ratio (SNR) for 1-year observations. Left: the SNR as a function of the initial PBH mass. The solid and dashed lines correspond to the cases with $\mathcal{P}_\zeta(\ln k)$ being the Gaussian with $\Delta = 1$ or the delta function, respectively. The orange, blue, vermilion, bluish-green, and reddish-purple lines correspond to CE, ET, BBO, DECIGO, and HLVK, respectively. Right: the contour plot of $\log_{10} \text{SNR}$ for CE (1 year) on the plane of $\log_{10}(M_{\text{PBH,ini}}/g)$ and $\log_{10} \Delta$. The contour lines denote $-4, -3, \dots, 3$ from left to right; the border between the pinkish and greenish regions corresponds to $\text{SNR} = 1$. See Appendix B for similar plots for ET, BBO, DECIGO, and HLVK.

It is defined as follows [103–105]

$$\text{SNR} = \sqrt{n_{\text{det}} t_{\text{obs}} \int_{f_{\text{min}}}^{f_{\text{max}}} df \left(\frac{\Omega_{\text{signal}}(f)}{\Omega_{\text{noise}}(f)} \right)^2}, \quad (10)$$

where n_{det} is the number of detectors in taking correlations, t_{obs} is the observational time, f_{max} and f_{min} are the maximum and minimum frequencies for each observation, and $\Omega_{\text{signal}}(f)$ and $\Omega_{\text{noise}}(f)$ are the signal and noise spectra, respectively.⁶ We set $n_{\text{det}} = 2, 2, 2, 1,$ and 4 for BBO, DECIGO, CE, ET, and HLVK, respectively.

The SNR in our setup is shown in Fig. 2. The left panel shows the SNR for each observation. The solid lines are for the lognormal $\mathcal{P}_\zeta(k)$ with $\Delta = 1$ whereas the dashed lines are for the delta-function $\mathcal{P}_\zeta(k)$. The orange, blue, vermilion, bluish-green, and reddish-purple lines correspond to CE, ET, BBO, DECIGO, and HLVK, respectively. As we discussed above, the signal can be more easily detected in the delta-function case because of the smaller power-law index of the IR tail. Since the space-based interferometers (DECIGO and BBO) sit in the deep IR, the increase of SNR of these observations is more significant from the lognormal case (solid lines) to the delta-function case (dashed lines).

The right panel of Fig. 2 is the contour plot of $\log_{10} \text{SNR}$ for CE on the plane spanned by $\log_{10}(M_{\text{PBH,ini}}/g)$ and $\log_{10} \Delta$. The corresponding contour plots for the other GW observations look qualitatively the same (see Appendix B). The figure again shows that sufficiently heavy memory-burdened PBH dark matter can be detected because of their relatively low-frequency induced GWs. Now, let us focus on the dependence on Δ . Since Δ controls the spectral width in terms of $\ln k$, the dependence of the SNR on Δ is significant for $\Delta \gtrsim 1$; the broader the spectra, the easier the observation is. For $\Delta \lesssim 1$, however, decreasing Δ does not narrow the GW spectrum because of the existence of the IR tail in the induced GW spectrum. Moreover,

⁶We use the data of the noise spectra available at <https://zenodo.org/records/3689582> associated with Ref. [77]. f_{min} and f_{max} are identified with the minimum and maximum frequencies in each data set.

the power-law index of the IR tail approaches 2 in the limit $\Delta \rightarrow 0$, so the sensitivity becomes better again toward the bottom of the figure. This explains the non-monotonic dependence of the SNR on Δ .

4 Tests of the scenario

Detection of the induced GWs with their intensity at the expected level (see Fig. 1) gives us affirmative information for the production of PBHs in the early Universe. However, it does not give us any hints on whether the produced PBHs have evaporated away or constitute dark matter at present. In this section, we discuss ways to confirm or exclude the scenario of the memory-burdened PBH dark matter.

4.1 Way to exclude the memory burden effect

If the induced GWs are observed with their intensity greater than the expected level, it means that the abundance of PBHs at their formation is greater than what is needed to explain the dark matter abundance. In the memory burden scenario, they lead to the overproduction of PBH dark matter. Even a signal a few times or dozens of percent greater than the expected level implies orders of magnitude too many PBHs. Therefore, if the induced GWs associated with light PBHs stronger than expected are observed, one can exclude the memory burden effect.

A way to avoid this conclusion is to dilute the overproduced memory-burdened PBH dark matter though this also dilutes the baryon asymmetry of the Universe if the generation of the baryon asymmetry took place earlier. In addition, the (incomplete) evaporation of the PBHs produces entropy and dilutes the baryon asymmetry further. The PBHs initially heavier than about 10^9 g are tightly constrained by the BBN. If one assumes that the baryon asymmetry of the Universe was produced sufficiently early (before PBH evaporation), the observed baryon-to-photon ratio puts an upper bound on the initial PBH abundance $\gamma\beta = (\rho_{\text{PBH}}/\rho_{\text{total}})|_{\text{ini}}$: $\beta' \lesssim 10^{-5} \left(\frac{10^9 \text{ g}}{M_{\text{PBH,ini}}} \right)$ for $M_{\text{PBH,ini}} < 10^9$ g, where $\beta' \equiv \gamma^{3/2} \left(\frac{106.75}{g_{*,\text{ini}}} \right)^{1/4} \left(\frac{0.67}{h} \right)^2 \beta$ (see Ref. [4] and references therein).⁷ Note that this bound can be evaded if the baryon asymmetry of the Universe is produced after the PBH evaporation and before the BBN.

In this way, one can constrain either the memory burden effect or the generation mechanism of the baryon asymmetry of the Universe if the too-strong induced GW signal is observed.

4.2 Ways to confirm the memory burden effect

Because the PBHs lighter than 10^{15} g evaporate away in the conventional scenario, the phenomenology of dark matter in the mass range $M_{\text{P}} \leq M \lesssim 10^{15}$ has not been studied as thoroughly as the heavier case $M \gtrsim 10^{15}$ g. Note also that the memory-burdened PBH in the memory burden phase typically has a mass of the order of its initial mass in contrast to the Planck-mass relics. Thus, the memory-burdened PBH dark matter and its properties such as mass and number density are in between those of particle dark matter and the conventional PBH dark matter without the memory burden effect. There may be unexplored rich phenomenology, and its thorough exploration is left for future work.

Optimistically, an indirect hint of PBH dark matter may be already found. In Ref. [106], it was found that the rate of the fast radio bursts (FRBs) increases in the presence of PBHs. The FRB rate asymptotes to a value comparable with observations [107, 108] for PBHs lighter than about 10^{22} g [106]. If we can exclude the conventional PBH mass range for the entirety of dark matter and other astrophysical explanations, we can argue that the memory-burdened PBHs are responsible for the observed FRB rate.

Next, we discuss the GWs originating from mergers of the memory-burdened PBH dark matter. This has been well studied in the context of explaining the LIGO/Virgo GW signals by

⁷The definition of β in this paper is different from that in Ref. [4]: $\gamma\beta_{\text{here}} = \beta_{\text{there}}$, where β_{here} is β in this paper (the formation probability) and β_{there} is β defined in Ref. [4] (the initial abundance).

PBH binary mergers. PBHs can form a binary in the early Universe [63, 109–111] as well as in the late Universe [112, 113]. For $30 M_\odot$ PBHs, the former mechanism is more effective [63, 111]. The merger rate per comoving volume approximately scales as $M_{\text{PBH}}^{-32/37}$ and M_{PBH}^0 for the early and late formation mechanisms, respectively, so the early-time binary formation mechanism is dominant also for PBHs lighter than $30 M_\odot$. The spectrum of the stochastic GW background from the superposition of mergers of light PBH binaries was discussed in the literature [50, 66, 114–116].⁸ It is obtained as follows:

$$\Omega_{\text{GW}}^{(\text{merger})}(\eta_0, f) = \frac{f}{\rho_c} \int_0^{z_{\text{sup}}} dz \frac{R(z)}{(1+z)H(z)} \frac{dE(f_s)}{df_s}, \quad (11)$$

where ρ_c is the critical density, z_{sup} is the upper bound of the redshift integral, R is the merger rate of PBH binaries per comoving volume, $f_s = (1+z)f$ is the frequency in the source frame, and dE/df_s is the GW spectrum from a merger in the source frame [123, 124]. The expressions of the upper bound z_{sup} , the merger rate R , and the energy spectrum dE/df_s are given in Appendix A. The spectrum of $\Omega_{\text{GW}}^{(\text{merger})}$ is shown in Fig. 3. The spectral shape is the same as the previous work in the literature. It follows the power-law $\Omega_{\text{GW}}^{(\text{merger})} \propto f^{2/3}$ [123–125] below the peak frequency. The peak frequency is $f_{\text{peak}} = 2 \times 10^{27} (M_{\text{PBH,ini}}/(10^{10} \text{ g}))^{-1}$ Hz, and the intensity at the peak is $\Omega_{\text{GW}}^{(\text{merger})}(f_{\text{peak}})h^2 = 6 \times 10^{-9} (M_{\text{PBH,ini}}/(10^{10} \text{ g}))^{5/37}$. Currently, there are no known methods to detect such extremely high-frequency GWs. For recent developments toward the detection of high-frequency GWs, see Refs. [126–140].

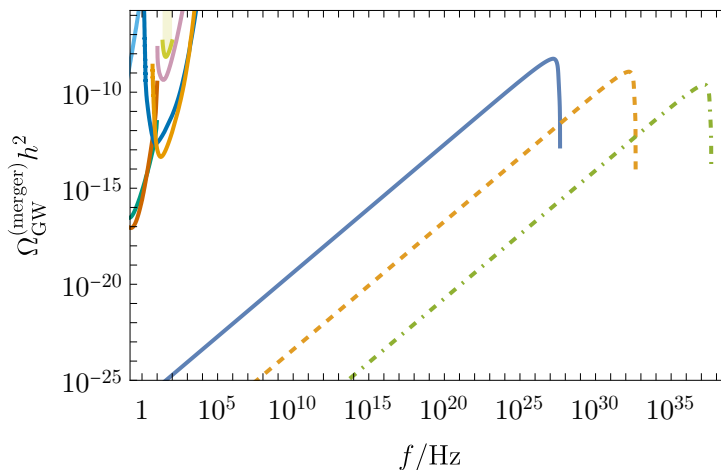


Figure 3: The spectra of the GWs from mergers of memory-burdened PBH binaries. From left to right, $M_{\text{PBH,ini}}/g = 10^{10}$ (the blue solid line), 10^5 (the orange dashed line), and 1 (the green dot-dashed line) with $M_{\text{PBH}} = M_{\text{PBH,ini}}/2$. The monochromatic mass function is assumed for simplicity. The same sensitivity curves as in Fig. 1 are also shown at the top left corner.

5 Conclusions

Despite active experimental programs, we do not have clear evidence of dark matter production at colliders or dark matter detection in direct and indirect detection experiments so far. If this situation continues, the nightmare scenario of dark matter, namely the scenario with only gravitationally interacting dark matter, will become important. Macroscopic dark matter is special in this context since they can offer some characteristic observational handles as in the case of the PBH scenario. One can imagine a pessimistic situation in which the conventional

⁸The same calculation applies to the supermassive black hole binaries if the environmental effect is negligible. If the evidence [117–120] of the GWs around nanohertz found by the worldwide pulsar timing array collaborations originates from the mergers of the supermassive black hole binaries, the environmental effect must be significant. See Refs. [121, 122] and references therein.

PBH dark matter mass window is observationally excluded. In this case, the PBHs beyond the semiclassical regime, namely the memory-burdened PBHs, become observationally more relevant in addition to their intrinsic importance. In this context, the induced GW signal associated with the memory-burdened PBH dark matter gives us important information: the mass of the PBHs. It can also be used for a consistency check of the memory-burdened PBH dark matter scenario.

We have discussed possibilities to observationally confirm, in principle, the memory burden effect working on PBH dark matter. In particular, the merger-originated GW signal is expected although the detailed form depends on the nonlinear dynamics of the memory-burdened PBH dark matter. The peak frequency is $f_{\text{peak}} = 2 \times 10^{27} (M_{\text{PBH, ini}}/(10^{10} \text{ g}))^{-1} \text{ Hz}$, which is far beyond the current limitation of the GW detection.

In contrast, we can also exclude the memory burden effect if the induced GWs associated with the light PBHs turn out to be stronger than expected, up to the non-minimal scenario that instead constrains the generation mechanism of the baryon asymmetry of the Universe. The observational constraint on the memory burden effect would be a valuable hint for black holes beyond the semi-classical regime and quantum gravity.

Taking into account the memory burden effect, we have studied the GWs induced by the enhanced primordial curvature perturbations that resulted in the formation of PBHs lighter than 10^{10} g . From the requirement that the PBH abundance explains the dark matter abundance, the intensity of the induced GWs is fixed precisely whereas the frequency of the induced GWs corresponds to the initial mass of the PBHs. The peak frequency of the induced GWs is $f_{\text{peak}} = 1 \times 10^3 (M_{\text{PBH}}/(10^{10} \text{ g}))^{-1/2} \text{ Hz}$ and the peak intensity is $\Omega_{\text{GW}}(f_{\text{peak}})h^2 = 7 \times 10^{-9}$. Although the frequency is high, there is the IR tail extending to lower frequencies. We have found that the induced GWs can be tested by future GW observations such as Cosmic Explorer. In conclusion, GWs give us clues about black holes beyond the semiclassical regime as well as about dark matter in the Universe.

Acknowledgment

K. K. and T. T. thank Sai Wang for discussions on the GWs from mergers of PBHs. This work was in part supported by MEXT KAKENHI Grants No. JP23KF0289, No. JP24H01825, No. JP24K07027 (K. K.), and No. 24H02244 (T. T. Y.). T. T. Y. was supported also by the Natural Science Foundation of China (NSFC) under Grant No. 12175134 as well as by World Premier International Research Center Initiative (WPI Initiative), MEXT, Japan. T. T.'s work was supported by the RIKEN TRIP initiative (RIKEN Quantum).

A Gravitational waves from mergers of PBH binaries

In this appendix, we summarize the formulas to calculate the spectrum of the GWs from mergers of PBH binaries. We follow Ref. [63] as well as Appendixes B and C of Ref. [115]. See also Appendix B of Ref. [50]. For simplicity, we assume a monochromatic PBH mass spectrum and the homogeneous spatial distribution of the PBHs. Also, we use the late-time PBH mass (in the memory burden regime) and do not take into account the time dependence of the PBH mass. This is justified since light PBHs quickly enter the memory burden regime.

For the convenience of the reader, we show Eq. (11) again:

$$\Omega_{\text{GW}}^{(\text{merger})}(\eta_0, f) = \frac{f}{\rho_c} \int_0^{z_{\text{sup}}} dz \frac{R(z)}{(1+z)H(z)} \frac{dE(f_s)}{df_s}.$$

The upper boundary of the integral is $z_{\text{sup}} = \min[z_{\text{max}}, (f_3/f) - 1]$ where z_{max} is the redshift at formation of PBHs, and f_3 is shortly given below. Practically, we can set $z_{\text{sup}} = (f_3/f) - 1$.

The merger rate per comoving volume is [63]

$$R(z) = \frac{f_{\text{PBH}} \Omega_{\text{CDM}} \rho_c}{M} \frac{dP_t}{dt}, \quad (12)$$

where the differential merger rate at time t for a PBH binary is [63]

$$\frac{dP_t}{dt} = \frac{3}{58t} \times \begin{cases} \left(\frac{t}{T}\right)^{3/37} - \left(\frac{t}{T}\right)^{3/8} & (t < t_c) \\ \left(\frac{t}{T}\right)^{3/8} \left(\left(\frac{t}{t_c}\right)^{-29/56} \left(\frac{4\pi f_{\text{PBH}}}{3}\right)^{-29/8} - 1 \right) & (t \geq t_c) \end{cases}, \quad (13)$$

where $T = \frac{729}{340\pi^2(1+z_{\text{eq}})^4(4\pi f_{\text{PBH}}^{16} M_{\text{PBH}}^5 \rho_c^4/3)^{1/3}}$ and $t_c = (4\pi f_{\text{PBH}}/3)^{37/3} T$.

The energy spectrum of the GWs at emission is [123, 124]

$$\frac{dE}{df_s}(f_s) = \frac{M_c^{5/3}}{12} \times \begin{cases} f_s^{-1/3} & (f_s \leq f_1) \\ f_1^{-1} f_s^{2/3} & (f_1 < f_s \leq f_2) \\ \frac{f_1^{-1} f_2^{-4/3} f_s^2}{\left(1 + \frac{4(f_s - f_2)^2}{\sigma^2}\right)^2} & (f_2 < f_s \leq f_3) \\ 0 & (f_3 < f_s) \end{cases}, \quad (14)$$

where $M_c = 2^{-1/3} M_{\text{PBH}}$ is the chirp mass, $f_1 = 0.4499 M_{\text{PBH}}^{-1}$, $f_2 = 1.026 M_{\text{PBH}}^{-1}$, $f_3 = 1.401 M_{\text{PBH}}^{-1}$ and $\sigma = 0.2381 M_{\text{PBH}}^{-1}$, where we have simplified the expressions assuming the monochromatic spectrum of the PBHs. Remember that we use $8\pi G = 1$ rather than $G = 1$.

Precisely speaking, the GW spectrum should follow the universal IR spectrum ($\Omega_{\text{GW}} \propto f^3$) well below the frequency corresponding to the inspiral frequency just after the binary formation [79]. Using the estimate of the IR cutoff frequency scale in Ref. [79], one can see that Fig. 3 is not affected in its plot region. Therefore, we neglect this effect for simplicity. For more on this point, see the discussions in Refs. [50, 79]. The spectrum of the merger-originated GWs is far below the observational sensitivity around and below the frequency range to which ground-based interferometers are sensitive.

B SNR contours for the other observations

In this appendix, we show the contour plots of the \log_{10} SNR for 1-year observations of the induced GWs for future GW observations: ET, BBO, DECIGO, and HLVK. See Fig. 4. The case of CE is shown on the right panel of Fig. 2.

References

- [1] S. W. Hawking, ‘‘Black hole explosions,’’ *Nature* **248** (1974) 30–31.
- [2] S. W. Hawking, ‘‘Particle Creation by Black Holes,’’ *Commun. Math. Phys.* **43** (1975) 199–220. [Erratum: *Commun.Math.Phys.* 46, 206 (1976)].
- [3] G. F. Chapline, ‘‘Cosmological effects of primordial black holes,’’ *Nature* **253** no. 5489, (1975) 251–252.
- [4] B. Carr, K. Kohri, Y. Sendouda, and J. Yokoyama, ‘‘Constraints on primordial black holes,’’ *Rept. Prog. Phys.* **84** no. 11, (2021) 116902, [arXiv:2002.12778 \[astro-ph.CO\]](#).
- [5] B. Carr and F. Kuhnel, ‘‘Primordial Black Holes as Dark Matter: Recent Developments,’’ *Ann. Rev. Nucl. Part. Sci.* **70** (2020) 355–394, [arXiv:2006.02838 \[astro-ph.CO\]](#).
- [6] A. M. Green and B. J. Kavanagh, ‘‘Primordial Black Holes as a dark matter candidate,’’ *J. Phys. G* **48** no. 4, (2021) 043001, [arXiv:2007.10722 \[astro-ph.CO\]](#).
- [7] A. Escrivà, F. Kuhnel, and Y. Tada, ‘‘Primordial Black Holes,’’ [arXiv:2211.05767 \[astro-ph.CO\]](#).
- [8] R. H. Price, ‘‘Nonspherical perturbations of relativistic gravitational collapse. 1. Scalar and gravitational perturbations,’’ *Phys. Rev. D* **5** (1972) 2419–2438.

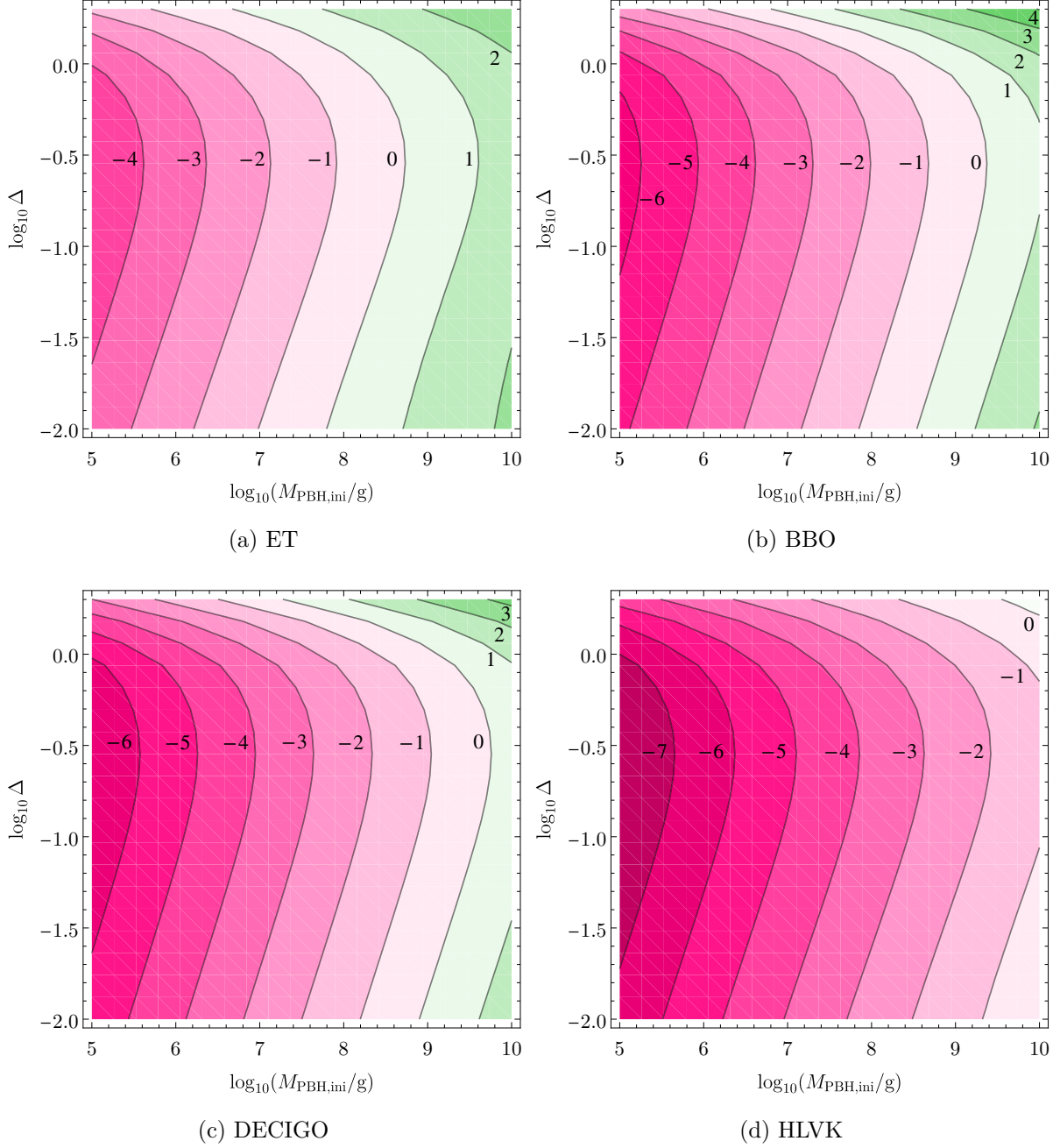


Figure 4: The contour plot of \log_{10} SNR for 1-year observation on the plane of $\log_{10}(M_{\text{PBH,ini}}/g)$ and $\log_{10} \Delta$. The border between the pinkish (low SNR) and greenish (high SNR) regions corresponds to $\text{SNR} = 1$ and the \log_{10} SNR changes by 1 for the adjacent contours. The corresponding figure for CE is shown on the right panel of Fig. 2

- [9] R. H. Price, “Nonspherical Perturbations of Relativistic Gravitational Collapse. II. Integer-Spin, Zero-Rest-Mass Fields,” *Phys. Rev. D* **5** (1972) 2439–2454.
- [10] S. W. Hawking, “Breakdown of Predictability in Gravitational Collapse,” *Phys. Rev. D* **14** (1976) 2460–2473.
- [11] G. Dvali and C. Gomez, “Black Hole’s Quantum N-Portrait,” *Fortsch. Phys.* **61** (2013) 742–767, [arXiv:1112.3359 \[hep-th\]](#).
- [12] G. Dvali and C. Gomez, “Black Holes as Critical Point of Quantum Phase Transition,” *Eur. Phys. J. C* **74** (2014) 2752, [arXiv:1207.4059 \[hep-th\]](#).
- [13] G. Dvali and C. Gomez, “Quantum Compositeness of Gravity: Black Holes, AdS and Inflation,” *JCAP* **01** (2014) 023, [arXiv:1312.4795 \[hep-th\]](#).
- [14] G. Dvali, “Non-Thermal Corrections to Hawking Radiation Versus the Information Paradox,” *Fortsch. Phys.* **64** (2016) 106–108, [arXiv:1509.04645 \[hep-th\]](#).
- [15] G. Dvali, “Critically excited states with enhanced memory and pattern recognition capacities in quantum brain networks: Lesson from black holes,” [arXiv:1711.09079 \[quant-ph\]](#).
- [16] G. Dvali, “Area law microstate entropy from criticality and spherical symmetry,” *Phys. Rev. D* **97** no. 10, (2018) 105005, [arXiv:1712.02233 \[hep-th\]](#).
- [17] G. Dvali, “Black Holes as Brains: Neural Networks with Area Law Entropy,” *Fortsch. Phys.* **66** no. 4, (2018) 1800007, [arXiv:1801.03918 \[hep-th\]](#).
- [18] G. Dvali, M. Michel, and S. Zell, “Finding Critical States of Enhanced Memory Capacity in Attractive Cold Bosons,” *EPJ Quant. Technol.* **6** (2019) 1, [arXiv:1805.10292 \[quant-ph\]](#).
- [19] G. Dvali, “A Microscopic Model of Holography: Survival by the Burden of Memory,” [arXiv:1810.02336 \[hep-th\]](#).
- [20] G. Dvali, L. Eisemann, M. Michel, and S. Zell, “Black hole metamorphosis and stabilization by memory burden,” *Phys. Rev. D* **102** no. 10, (2020) 103523, [arXiv:2006.00011 \[hep-th\]](#).
- [21] G. Dvali, J. S. Valbuena-Bermúdez, and M. Zantedeschi, “Memory Burden Effect in Black Holes and Solitons: Implications for PBH,” [arXiv:2405.13117 \[hep-th\]](#).
- [22] A. Alexandre, G. Dvali, and E. Koutsangelas, “New Mass Window for Primordial Black Holes as Dark Matter from Memory Burden Effect,” [arXiv:2402.14069 \[hep-ph\]](#).
- [23] V. Thoss, A. Burkert, and K. Kohri, “Breakdown of Hawking Evaporation opens new Mass Window for Primordial Black Holes as Dark Matter Candidate,” [arXiv:2402.17823 \[astro-ph.CO\]](#).
- [24] M. R. Haque, S. Maity, D. Maity, and Y. Mambrini, “Quantum effects on the evaporation of PBHs: contributions to dark matter,” [arXiv:2404.16815 \[hep-ph\]](#).
- [25] B. Barman, M. R. Haque, and O. Zapata, “Gravitational wave signatures of cogenesis from a burdened PBH,” [arXiv:2405.15858 \[astro-ph.CO\]](#).
- [26] R. Bousso, “A Covariant entropy conjecture,” *JHEP* **07** (1999) 004, [arXiv:hep-th/9905177](#).
- [27] P. Chen, Y. C. Ong, and D.-h. Yeom, “Black Hole Remnants and the Information Loss Paradox,” *Phys. Rept.* **603** (2015) 1–45, [arXiv:1412.8366 \[gr-qc\]](#).

- [28] G. Domènech and M. Sasaki, “Gravitational wave hints black hole remnants as dark matter,” *Class. Quant. Grav.* **40** no. 17, (2023) 177001, [arXiv:2303.07661 \[gr-qc\]](#).
- [29] B. J. Carr, K. Kohri, Y. Sendouda, and J. Yokoyama, “New cosmological constraints on primordial black holes,” *Phys. Rev. D* **81** (2010) 104019, [arXiv:0912.5297 \[astro-ph.CO\]](#).
- [30] S. Hawking, “Gravitationally collapsed objects of very low mass,” *Mon. Not. Roy. Astron. Soc.* **152** (1971) 75.
- [31] B. J. Carr and S. W. Hawking, “Black holes in the early Universe,” *Mon. Not. Roy. Astron. Soc.* **168** (1974) 399–415.
- [32] **BICEP, Keck** Collaboration, P. A. R. Ade *et al.*, “Improved Constraints on Primordial Gravitational Waves using Planck, WMAP, and BICEP/Keck Observations through the 2018 Observing Season,” *Phys. Rev. Lett.* **127** no. 15, (2021) 151301, [arXiv:2110.00483 \[astro-ph.CO\]](#).
- [33] M. Tristram *et al.*, “Improved limits on the tensor-to-scalar ratio using BICEP and Planck data,” *Phys. Rev. D* **105** no. 8, (2022) 083524, [arXiv:2112.07961 \[astro-ph.CO\]](#).
- [34] D. Paoletti, F. Finelli, J. Valiviita, and M. Hazumi, “Planck and BICEP/Keck Array 2018 constraints on primordial gravitational waves and perspectives for future B-mode polarization measurements,” *Phys. Rev. D* **106** no. 8, (2022) 083528, [arXiv:2208.10482 \[astro-ph.CO\]](#).
- [35] **Planck** Collaboration, N. Aghanim *et al.*, “Planck 2018 results. VI. Cosmological parameters,” *Astron. Astrophys.* **641** (2020) A6, [arXiv:1807.06209 \[astro-ph.CO\]](#). [Erratum: *Astron. Astrophys.* 652, C4 (2021)].
- [36] **Planck** Collaboration, Y. Akrami *et al.*, “Planck 2018 results. X. Constraints on inflation,” *Astron. Astrophys.* **641** (2020) A10, [arXiv:1807.06211 \[astro-ph.CO\]](#).
- [37] R. Saito and J. Yokoyama, “Gravitational wave background as a probe of the primordial black hole abundance,” *Phys. Rev. Lett.* **102** (2009) 161101, [arXiv:0812.4339 \[astro-ph\]](#). [Erratum: *Phys. Rev. Lett.* 107, 069901 (2011)].
- [38] R. Saito and J. Yokoyama, “Gravitational-Wave Constraints on the Abundance of Primordial Black Holes,” *Prog. Theor. Phys.* **123** (2010) 867–886, [arXiv:0912.5317 \[astro-ph.CO\]](#). [Erratum: *Prog. Theor. Phys.* 126, 351–352 (2011)].
- [39] K. Tomita, “Non-Linear Theory of Gravitational Instability in the Expanding Universe,” *Progress of Theoretical Physics* **37** no. 5, (May, 1967) 831–846.
- [40] S. Matarrese, O. Pantano, and D. Saez, “A General relativistic approach to the nonlinear evolution of collisionless matter,” *Phys. Rev. D* **47** (1993) 1311–1323.
- [41] S. Matarrese, O. Pantano, and D. Saez, “General relativistic dynamics of irrotational dust: Cosmological implications,” *Phys. Rev. Lett.* **72** (1994) 320–323, [arXiv:astro-ph/9310036](#).
- [42] S. Matarrese, S. Mollerach, and M. Bruni, “Second order perturbations of the Einstein-de Sitter universe,” *Phys. Rev. D* **58** (1998) 043504, [arXiv:astro-ph/9707278](#).
- [43] K. N. Ananda, C. Clarkson, and D. Wands, “The Cosmological gravitational wave background from primordial density perturbations,” *Phys. Rev. D* **75** (2007) 123518, [arXiv:gr-qc/0612013](#).

- [44] D. Baumann, P. J. Steinhardt, K. Takahashi, and K. Ichiki, “Gravitational Wave Spectrum Induced by Primordial Scalar Perturbations,” *Phys. Rev. D* **76** (2007) 084019, [arXiv:hep-th/0703290](#).
- [45] LISA Collaboration, P. Amaro-Seoane *et al.*, “Laser Interferometer Space Antenna,” [arXiv:1702.00786 \[astro-ph.IM\]](#).
- [46] J. Baker *et al.*, “The Laser Interferometer Space Antenna: Unveiling the Millihertz Gravitational Wave Sky,” [arXiv:1907.06482 \[astro-ph.IM\]](#).
- [47] S. Balaji, G. Domènech, G. Franciolini, A. Ganz, and J. Tränkle, “Probing modified Hawking evaporation with gravitational waves from the primordial black hole dominated universe,” [arXiv:2403.14309 \[gr-qc\]](#).
- [48] N. Bhaumik, M. R. Haque, R. K. Jain, and M. Lewicki, “Memory burden effect mimics reheating signatures on SGWB from ultra-low mass PBH domination,” [arXiv:2409.04436 \[astro-ph.CO\]](#).
- [49] K. Inomata, K. Kohri, T. Nakama, and T. Terada, “Enhancement of Gravitational Waves Induced by Scalar Perturbations due to a Sudden Transition from an Early Matter Era to the Radiation Era,” *Phys. Rev. D* **100** (2019) 043532, [arXiv:1904.12879 \[astro-ph.CO\]](#). [Erratum: *Phys.Rev.D* 108, 049901 (2023)].
- [50] K. Inomata, M. Kawasaki, K. Mukaida, T. Terada, and T. T. Yanagida, “Gravitational Wave Production right after a Primordial Black Hole Evaporation,” *Phys. Rev. D* **101** no. 12, (2020) 123533, [arXiv:2003.10455 \[astro-ph.CO\]](#).
- [51] T. Papanikolaou, V. Vennin, and D. Langlois, “Gravitational waves from a universe filled with primordial black holes,” *JCAP* **03** (2021) 053, [arXiv:2010.11573 \[astro-ph.CO\]](#).
- [52] G. Domènech, C. Lin, and M. Sasaki, “Gravitational wave constraints on the primordial black hole dominated early universe,” *JCAP* **04** (2021) 062, [arXiv:2012.08151 \[gr-qc\]](#). [Erratum: *JCAP* 11, E01 (2021)].
- [53] K. Inomata, K. Kohri, T. Nakama, and T. Terada, “Gravitational Waves Induced by Scalar Perturbations during a Gradual Transition from an Early Matter Era to the Radiation Era,” *JCAP* **10** (2019) 071, [arXiv:1904.12878 \[astro-ph.CO\]](#). [Erratum: *JCAP* 08, E01 (2023)].
- [54] T. Papanikolaou, “Gravitational waves induced from primordial black hole fluctuations: the effect of an extended mass function,” *JCAP* **10** (2022) 089, [arXiv:2207.11041 \[astro-ph.CO\]](#).
- [55] K. Harigaya, K. Inomata, and T. Terada, “Gravitational wave production from axion rotations right after a transition to kination,” *Phys. Rev. D* **108** no. 8, (2023) L081303, [arXiv:2305.14242 \[hep-ph\]](#).
- [56] M. Pearce, L. Pearce, G. White, and C. Balazs, “Gravitational Wave Signals From Early Matter Domination: Interpolating Between Fast and Slow Transitions,” [arXiv:2311.12340 \[astro-ph.CO\]](#).
- [57] K. Ando, K. Inomata, and M. Kawasaki, “Primordial black holes and uncertainties in the choice of the window function,” *Phys. Rev. D* **97** no. 10, (2018) 103528, [arXiv:1802.06393 \[astro-ph.CO\]](#).
- [58] S. Young, “The primordial black hole formation criterion re-examined: Parametrisation, timing and the choice of window function,” *Int. J. Mod. Phys. D* **29** no. 02, (2019) 2030002, [arXiv:1905.01230 \[astro-ph.CO\]](#).

- [59] C.-M. Yoo, T. Harada, S. Hirano, and K. Kohri, “Abundance of Primordial Black Holes in Peak Theory for an Arbitrary Power Spectrum,” *PTEP* **2021** no. 1, (2021) 013E02, [arXiv:2008.02425 \[astro-ph.CO\]](#). [Erratum: PTEP 2024, 049203 (2024)].
- [60] V. De Luca, A. Kehagias, and A. Riotto, “How well do we know the primordial black hole abundance: The crucial role of nonlinearities when approaching the horizon,” *Phys. Rev. D* **108** no. 6, (2023) 063531, [arXiv:2307.13633 \[astro-ph.CO\]](#).
- [61] G. Franciolini, A. Iannicari, A. Kehagias, D. Perrone, and A. Riotto, “Renormalized Primordial Black Holes,” [arXiv:2311.03239 \[astro-ph.CO\]](#).
- [62] A. Iannicari, A. J. Iovino, A. Kehagias, D. Perrone, and A. Riotto, “The Primordial Black Hole Abundance: The Broader, the Better,” [arXiv:2402.11033 \[astro-ph.CO\]](#).
- [63] M. Sasaki, T. Suyama, T. Tanaka, and S. Yokoyama, “Primordial black holes—perspectives in gravitational wave astronomy,” *Class. Quant. Grav.* **35** no. 6, (2018) 063001, [arXiv:1801.05235 \[astro-ph.CO\]](#).
- [64] K. Inomata, M. Kawasaki, K. Mukaida, Y. Tada, and T. T. Yanagida, “Inflationary Primordial Black Holes as All Dark Matter,” *Phys. Rev. D* **96** no. 4, (2017) 043504, [arXiv:1701.02544 \[astro-ph.CO\]](#).
- [65] **NANOGrav** Collaboration, A. Afzal *et al.*, “The NANOGrav 15 yr Data Set: Search for Signals from New Physics,” *Astrophys. J. Lett.* **951** no. 1, (2023) L11, [arXiv:2306.16219 \[astro-ph.HE\]](#).
- [66] K. Inomata, K. Kohri, and T. Terada, “Detected stochastic gravitational waves and subsolar-mass primordial black holes,” *Phys. Rev. D* **109** no. 6, (2024) 063506, [arXiv:2306.17834 \[astro-ph.CO\]](#).
- [67] B. J. Carr, “The Primordial black hole mass spectrum,” *Astrophys. J.* **201** (1975) 1–19.
- [68] W. H. Press and P. Schechter, “Formation of galaxies and clusters of galaxies by selfsimilar gravitational condensation,” *Astrophys. J.* **187** (1974) 425–438.
- [69] D. Hooper, G. Krnjaic, and S. D. McDermott, “Dark Radiation and Superheavy Dark Matter from Black Hole Domination,” *JHEP* **08** (2019) 001, [arXiv:1905.01301 \[hep-ph\]](#).
- [70] J. H. MacGibbon and B. R. Webber, “Quark and gluon jet emission from primordial black holes: The instantaneous spectra,” *Phys. Rev. D* **41** (1990) 3052–3079.
- [71] J. H. MacGibbon, “Quark and gluon jet emission from primordial black holes. 2. The Lifetime emission,” *Phys. Rev. D* **44** (1991) 376–392.
- [72] J. D. Bekenstein, “Black holes and the second law,” *Lett. Nuovo Cim.* **4** (1972) 737–740.
- [73] J. M. Bardeen, B. Carter, and S. W. Hawking, “The Four laws of black hole mechanics,” *Commun. Math. Phys.* **31** (1973) 161–170.
- [74] K. Saikawa and S. Shirai, “Primordial gravitational waves, precisely: The role of thermodynamics in the Standard Model,” *JCAP* **05** (2018) 035, [arXiv:1803.01038 \[hep-ph\]](#).
- [75] J. R. Espinosa, D. Racco, and A. Riotto, “A Cosmological Signature of the SM Higgs Instability: Gravitational Waves,” *JCAP* **09** (2018) 012, [arXiv:1804.07732 \[hep-ph\]](#).
- [76] K. Kohri and T. Terada, “Semianalytic calculation of gravitational wave spectrum nonlinearly induced from primordial curvature perturbations,” *Phys. Rev. D* **97** no. 12, (2018) 123532, [arXiv:1804.08577 \[gr-qc\]](#).

- [77] K. Schmitz, “New Sensitivity Curves for Gravitational-Wave Signals from Cosmological Phase Transitions,” *JHEP* **01** (2021) 097, [arXiv:2002.04615 \[hep-ph\]](#).
- [78] C. Yuan, Z.-C. Chen, and Q.-G. Huang, “Log-dependent slope of scalar induced gravitational waves in the infrared regions,” *Phys. Rev. D* **101** no. 4, (2020) 043019, [arXiv:1910.09099 \[astro-ph.CO\]](#).
- [79] R.-G. Cai, S. Pi, and M. Sasaki, “Universal infrared scaling of gravitational wave background spectra,” *Phys. Rev. D* **102** no. 8, (2020) 083528, [arXiv:1909.13728 \[astro-ph.CO\]](#).
- [80] S. Pi and M. Sasaki, “Gravitational Waves Induced by Scalar Perturbations with a Lognormal Peak,” *JCAP* **09** (2020) 037, [arXiv:2005.12306 \[gr-qc\]](#).
- [81] N. Seto, S. Kawamura, and T. Nakamura, “Possibility of direct measurement of the acceleration of the universe using 0.1-Hz band laser interferometer gravitational wave antenna in space,” *Phys. Rev. Lett.* **87** (2001) 221103, [arXiv:astro-ph/0108011](#).
- [82] K. Yagi and N. Seto, “Detector configuration of DECIGO/BBO and identification of cosmological neutron-star binaries,” *Phys. Rev. D* **83** (2011) 044011, [arXiv:1101.3940 \[astro-ph.CO\]](#). [Erratum: *Phys.Rev.D* 95, 109901 (2017)].
- [83] S. Isoyama, H. Nakano, and T. Nakamura, “Multiband Gravitational-Wave Astronomy: Observing binary inspirals with a decihertz detector, B-DECIGO,” *PTEP* **2018** no. 7, (2018) 073E01, [arXiv:1802.06977 \[gr-qc\]](#).
- [84] S. Kawamura *et al.*, “Current status of space gravitational wave antenna DECIGO and B-DECIGO,” *PTEP* **2021** no. 5, (2021) 05A105, [arXiv:2006.13545 \[gr-qc\]](#).
- [85] J. Crowder and N. J. Cornish, “Beyond LISA: Exploring future gravitational wave missions,” *Phys. Rev. D* **72** (2005) 083005, [arXiv:gr-qc/0506015](#).
- [86] V. Corbin and N. J. Cornish, “Detecting the cosmic gravitational wave background with the big bang observer,” *Class. Quant. Grav.* **23** (2006) 2435–2446, [arXiv:gr-qc/0512039](#).
- [87] G. M. Harry, P. Fritschel, D. A. Shaddock, W. Folkner, and E. S. Phinney, “Laser interferometry for the big bang observer,” *Class. Quant. Grav.* **23** (2006) 4887–4894. [Erratum: *Class.Quant.Grav.* 23, 7361 (2006)].
- [88] **KAGRA, Virgo, LIGO Scientific** Collaboration, R. Abbott *et al.*, “Upper limits on the isotropic gravitational-wave background from Advanced LIGO and Advanced Virgo’s third observing run,” *Phys. Rev. D* **104** no. 2, (2021) 022004, [arXiv:2101.12130 \[gr-qc\]](#).
- [89] **LIGO Scientific** Collaboration, G. M. Harry, “Advanced LIGO: The next generation of gravitational wave detectors,” *Class. Quant. Grav.* **27** (2010) 084006.
- [90] **LIGO Scientific** Collaboration, J. Aasi *et al.*, “Advanced LIGO,” *Class. Quant. Grav.* **32** (2015) 074001, [arXiv:1411.4547 \[gr-qc\]](#).
- [91] **VIRGO** Collaboration, F. Acernese *et al.*, “Advanced Virgo: a second-generation interferometric gravitational wave detector,” *Class. Quant. Grav.* **32** no. 2, (2015) 024001, [arXiv:1408.3978 \[gr-qc\]](#).
- [92] **KAGRA** Collaboration, K. Somiya, “Detector configuration of KAGRA: The Japanese cryogenic gravitational-wave detector,” *Class. Quant. Grav.* **29** (2012) 124007, [arXiv:1111.7185 \[gr-qc\]](#).

- [93] **KAGRA** Collaboration, Y. Aso, Y. Michimura, K. Somiya, M. Ando, O. Miyakawa, T. Sekiguchi, D. Tatsumi, and H. Yamamoto, “Interferometer design of the KAGRA gravitational wave detector,” *Phys. Rev. D* **88** no. 4, (2013) 043007, [arXiv:1306.6747 \[gr-qc\]](#).
- [94] **KAGRA** Collaboration, T. Akutsu *et al.*, “KAGRA: 2.5 Generation Interferometric Gravitational Wave Detector,” *Nature Astron.* **3** no. 1, (2019) 35–40, [arXiv:1811.08079 \[gr-qc\]](#).
- [95] **KAGRA** Collaboration, T. Akutsu *et al.*, “First cryogenic test operation of underground km-scale gravitational-wave observatory KAGRA,” *Class. Quant. Grav.* **36** no. 16, (2019) 165008, [arXiv:1901.03569 \[astro-ph.IM\]](#).
- [96] Y. Michimura *et al.*, “Prospects for improving the sensitivity of KAGRA gravitational wave detector,” in *15th Marcel Grossmann Meeting on Recent Developments in Theoretical and Experimental General Relativity, Astrophysics, and Relativistic Field Theories*. 6, 2019. [arXiv:1906.02866 \[gr-qc\]](#).
- [97] M. Punturo *et al.*, “The Einstein Telescope: A third-generation gravitational wave observatory,” *Class. Quant. Grav.* **27** (2010) 194002.
- [98] S. Hild *et al.*, “Sensitivity Studies for Third-Generation Gravitational Wave Observatories,” *Class. Quant. Grav.* **28** (2011) 094013, [arXiv:1012.0908 \[gr-qc\]](#).
- [99] B. Sathyaprakash *et al.*, “Scientific Objectives of Einstein Telescope,” *Class. Quant. Grav.* **29** (2012) 124013, [arXiv:1206.0331 \[gr-qc\]](#). [Erratum: *Class. Quant. Grav.* 30, 079501 (2013)].
- [100] M. Maggiore *et al.*, “Science Case for the Einstein Telescope,” *JCAP* **03** (2020) 050, [arXiv:1912.02622 \[astro-ph.CO\]](#).
- [101] **LIGO Scientific** Collaboration, B. P. Abbott *et al.*, “Exploring the Sensitivity of Next Generation Gravitational Wave Detectors,” *Class. Quant. Grav.* **34** no. 4, (2017) 044001, [arXiv:1607.08697 \[astro-ph.IM\]](#).
- [102] D. Reitze *et al.*, “Cosmic Explorer: The U.S. Contribution to Gravitational-Wave Astronomy beyond LIGO,” *Bull. Am. Astron. Soc.* **51** no. 7, (2019) 035, [arXiv:1907.04833 \[astro-ph.IM\]](#). <https://baas.aas.org/pub/2020n7i035>.
- [103] M. Maggiore, “Gravitational wave experiments and early universe cosmology,” *Phys. Rept.* **331** (2000) 283–367, [arXiv:gr-qc/9909001](#).
- [104] B. Allen, “The Stochastic gravity wave background: Sources and detection,” in *Les Houches School of Physics: Astrophysical Sources of Gravitational Radiation*, pp. 373–417. 4, 1996. [arXiv:gr-qc/9604033](#).
- [105] B. Allen and J. D. Romano, “Detecting a stochastic background of gravitational radiation: Signal processing strategies and sensitivities,” *Phys. Rev. D* **59** (1999) 102001, [arXiv:gr-qc/9710117](#).
- [106] K. Kainulainen, S. Nurmi, E. D. Schiappacasse, and T. T. Yanagida, “Can primordial black holes as all dark matter explain fast radio bursts?,” *Phys. Rev. D* **104** no. 12, (2021) 123033, [arXiv:2108.08717 \[astro-ph.HE\]](#).
- [107] D. J. Champion *et al.*, “Five new fast radio bursts from the HTRU high-latitude survey at Parkes: first evidence for two-component bursts,” *Mon. Not. Roy. Astron. Soc.* **460** no. 1, (2016) L30–L34, [arXiv:1511.07746 \[astro-ph.HE\]](#).

- [108] E. Petroff, J. W. T. Hessels, and D. R. Lorimer, “Fast Radio Bursts,” *Astron. Astrophys. Rev.* **27** no. 1, (2019) 4, [arXiv:1904.07947 \[astro-ph.HE\]](#).
- [109] T. Nakamura, M. Sasaki, T. Tanaka, and K. S. Thorne, “Gravitational waves from coalescing black hole MACHO binaries,” *Astrophys. J. Lett.* **487** (1997) L139–L142, [arXiv:astro-ph/9708060](#).
- [110] K. Ioka, T. Chiba, T. Tanaka, and T. Nakamura, “Black hole binary formation in the expanding universe: Three body problem approximation,” *Phys. Rev. D* **58** (1998) 063003, [arXiv:astro-ph/9807018](#).
- [111] M. Sasaki, T. Suyama, T. Tanaka, and S. Yokoyama, “Primordial Black Hole Scenario for the Gravitational-Wave Event GW150914,” *Phys. Rev. Lett.* **117** no. 6, (2016) 061101, [arXiv:1603.08338 \[astro-ph.CO\]](#). [Erratum: *Phys.Rev.Lett.* 121, 059901 (2018)].
- [112] S. Bird, I. Cholis, J. B. Muñoz, Y. Ali-Haïmoud, M. Kamionkowski, E. D. Kovetz, A. Raccanelli, and A. G. Riess, “Did LIGO detect dark matter?,” *Phys. Rev. Lett.* **116** no. 20, (2016) 201301, [arXiv:1603.00464 \[astro-ph.CO\]](#).
- [113] S. Clesse and J. García-Bellido, “The clustering of massive Primordial Black Holes as Dark Matter: measuring their mass distribution with Advanced LIGO,” *Phys. Dark Univ.* **15** (2017) 142–147, [arXiv:1603.05234 \[astro-ph.CO\]](#).
- [114] S. Wang, Y.-F. Wang, Q.-G. Huang, and T. G. F. Li, “Constraints on the Primordial Black Hole Abundance from the First Advanced LIGO Observation Run Using the Stochastic Gravitational-Wave Background,” *Phys. Rev. Lett.* **120** no. 19, (2018) 191102, [arXiv:1610.08725 \[astro-ph.CO\]](#).
- [115] S. Wang, T. Terada, and K. Kohri, “Prospective constraints on the primordial black hole abundance from the stochastic gravitational-wave backgrounds produced by coalescing events and curvature perturbations,” *Phys. Rev. D* **99** no. 10, (2019) 103531, [arXiv:1903.05924 \[astro-ph.CO\]](#). [Erratum: *Phys.Rev.D* 101, 069901 (2020)].
- [116] K. Kohri and T. Terada, “Solar-Mass Primordial Black Holes Explain NANOGrav Hint of Gravitational Waves,” *Phys. Lett. B* **813** (2021) 136040, [arXiv:2009.11853 \[astro-ph.CO\]](#).
- [117] **NANOGrav** Collaboration, G. Agazie *et al.*, “The NANOGrav 15 yr Data Set: Evidence for a Gravitational-wave Background,” *Astrophys. J. Lett.* **951** no. 1, (2023) L8, [arXiv:2306.16213 \[astro-ph.HE\]](#).
- [118] **EPTA, InPTA:** Collaboration, J. Antoniadis *et al.*, “The second data release from the European Pulsar Timing Array - III. Search for gravitational wave signals,” *Astron. Astrophys.* **678** (2023) A50, [arXiv:2306.16214 \[astro-ph.HE\]](#).
- [119] D. J. Reardon *et al.*, “Search for an Isotropic Gravitational-wave Background with the Parkes Pulsar Timing Array,” *Astrophys. J. Lett.* **951** no. 1, (2023) L6, [arXiv:2306.16215 \[astro-ph.HE\]](#).
- [120] H. Xu *et al.*, “Searching for the Nano-Hertz Stochastic Gravitational Wave Background with the Chinese Pulsar Timing Array Data Release I,” *Res. Astron. Astrophys.* **23** no. 7, (2023) 075024, [arXiv:2306.16216 \[astro-ph.HE\]](#).
- [121] **NANOGrav** Collaboration, G. Agazie *et al.*, “The NANOGrav 15 yr Data Set: Constraints on Supermassive Black Hole Binaries from the Gravitational-wave Background,” *Astrophys. J. Lett.* **952** no. 2, (2023) L37, [arXiv:2306.16220 \[astro-ph.HE\]](#).

- [122] **EPTA, InPTA** Collaboration, J. Antoniadis *et al.*, “The second data release from the European Pulsar Timing Array - IV. Implications for massive black holes, dark matter, and the early Universe,” *Astron. Astrophys.* **685** (2024) A94, [arXiv:2306.16227 \[astro-ph.CO\]](#).
- [123] P. Ajith *et al.*, “A Template bank for gravitational waveforms from coalescing binary black holes. I. Non-spinning binaries,” *Phys. Rev. D* **77** (2008) 104017, [arXiv:0710.2335 \[gr-qc\]](#). [Erratum: *Phys.Rev.D* 79, 129901 (2009)].
- [124] P. Ajith *et al.*, “Inspiral-merger-ringdown waveforms for black-hole binaries with non-precessing spins,” *Phys. Rev. Lett.* **106** (2011) 241101, [arXiv:0909.2867 \[gr-qc\]](#).
- [125] E. S. Phinney, “A Practical theorem on gravitational wave backgrounds,” [arXiv:astro-ph/0108028](#).
- [126] A. D. Dolgov and D. Ejlli, “Conversion of relic gravitational waves into photons in cosmological magnetic fields,” *JCAP* **12** (2012) 003, [arXiv:1211.0500 \[gr-qc\]](#).
- [127] V. Domcke and C. Garcia-Cely, “Potential of radio telescopes as high-frequency gravitational wave detectors,” *Phys. Rev. Lett.* **126** no. 2, (2021) 021104, [arXiv:2006.01161 \[astro-ph.CO\]](#).
- [128] A. Ejlli, D. Ejlli, A. M. Cruise, G. Pisano, and H. Grote, “Upper limits on the amplitude of ultra-high-frequency gravitational waves from graviton to photon conversion,” *Eur. Phys. J. C* **79** no. 12, (2019) 1032, [arXiv:1908.00232 \[gr-qc\]](#).
- [129] N. Aggarwal *et al.*, “Challenges and opportunities of gravitational-wave searches at MHz to GHz frequencies,” *Living Rev. Rel.* **24** no. 1, (2021) 4, [arXiv:2011.12414 \[gr-qc\]](#).
- [130] N. Herman, A. Füzfa, L. Lehoucq, and S. Clesse, “Detecting planetary-mass primordial black holes with resonant electromagnetic gravitational-wave detectors,” *Phys. Rev. D* **104** no. 2, (2021) 023524, [arXiv:2012.12189 \[gr-qc\]](#).
- [131] A. Berlin, D. Blas, R. Tito D’Agnolo, S. A. R. Ellis, R. Harnik, Y. Kahn, and J. Schütte-Engel, “Detecting high-frequency gravitational waves with microwave cavities,” *Phys. Rev. D* **105** no. 11, (2022) 116011, [arXiv:2112.11465 \[hep-ph\]](#).
- [132] V. Domcke, C. Garcia-Cely, and N. L. Rodd, “Novel Search for High-Frequency Gravitational Waves with Low-Mass Axion Haloscopes,” *Phys. Rev. Lett.* **129** no. 4, (2022) 041101, [arXiv:2202.00695 \[hep-ph\]](#).
- [133] M. E. Tobar, C. A. Thomson, W. M. Campbell, A. Quiskamp, J. F. Bourhill, B. T. McAllister, E. N. Ivanov, and M. Goryachev, “Comparing Instrument Spectral Sensitivity of Dissimilar Electromagnetic Haloscopes to Axion Dark Matter and High Frequency Gravitational Waves,” *Symmetry* **14** no. 10, (2022) 2165, [arXiv:2209.03004 \[physics.ins-det\]](#).
- [134] D. Ahn, Y.-B. Bae, S. H. Im, and C. Park, “Electromagnetic field in a cavity induced by gravitational waves,” [arXiv:2312.09550 \[gr-qc\]](#).
- [135] A. Ito, T. Ikeda, K. Miuchi, and J. Soda, “Probing GHz gravitational waves with graviton–magnon resonance,” *Eur. Phys. J. C* **80** no. 3, (2020) 179, [arXiv:1903.04843 \[gr-qc\]](#).
- [136] A. Ito and J. Soda, “A formalism for magnon gravitational wave detectors,” *Eur. Phys. J. C* **80** no. 6, (2020) 545, [arXiv:2004.04646 \[gr-qc\]](#).
- [137] A. Ito and J. Soda, “Exploring high-frequency gravitational waves with magnons,” *Eur. Phys. J. C* **83** no. 8, (2023) 766, [arXiv:2212.04094 \[gr-qc\]](#).

- [138] A. Ito, K. Kohri, and K. Nakayama, “Probing high frequency gravitational waves with pulsars,” *Phys. Rev. D* **109** no. 6, (2024) 063026, [arXiv:2305.13984 \[gr-qc\]](#).
- [139] T. Liu, J. Ren, and C. Zhang, “Limits on High-Frequency Gravitational Waves in Planetary Magnetospheres,” *Phys. Rev. Lett.* **132** no. 13, (2024) 131402, [arXiv:2305.01832 \[hep-ph\]](#).
- [140] A. Ito, K. Kohri, and K. Nakayama, “Gravitational Wave Search through Electromagnetic Telescopes,” *PTEP* **2024** no. 2, (2024) 023E03, [arXiv:2309.14765 \[gr-qc\]](#).